AGU PUBLICATIONS

Geophysical Research Letters

RESEARCH LETTER
10.1002/2013GL059081

Key Points:
- A 1200-year drought reconstruction for the Swiss Alps was established
- The tree-ring carbon isotope ratios at the site are highly moisture-sensitive
- The data fill a gap in our knowledge about medieval hydroclimate

Supporting Information:
- Readme
- Table S1

Correspondence to:
M. Saurer,
matthias.saurer@psi.ch

Citation:
Kress, A., S. Hangartner, H. Bugmann, U. Büntgen, D. C. Frank, M. Leuenberger, R. T. W. Siegwolf, and M. Saurer (2014), Swiss tree rings reveal warm and wet summers during medieval times, *Geophys. Res. Lett.*, *41*, 1732–1737, doi:10.1002/2013GL059081.

Received 19 DEC 2013
Accepted 23 JAN 2014
Accepted article online 27 JAN 2014
Published online 12 MAR 2014

Swiss tree rings reveal warm and wet summers during medieval times

Anne Kress[1,2], Sarah Hangartner[3], Harald Bugmann[4], Ulf Büntgen[5,6,7], David C. Frank[5,6], Markus Leuenberger[3], Rolf T.W. Siegwolf[1], and Matthias Saurer[1]

[1]Laboratory of Atmospheric Chemistry, Paul Scherrer Institute, Villigen, Switzerland, [2]Faculty of Forestry, University of Applied Sciences Weihenstephan-Triesdorf, Freising, Germany, [3]Climate and Environmental Physics, University of Bern, Bern, Switzerland, [4]Forest Ecology, Department of Environmental Systems Sciences, ETH Zürich, Zürich, Switzerland, [5]Swiss Federal Research Institute WSL, Birmensdorf, Switzerland, [6]Oeschger Centre for Climate Change Research, University of Bern, Bern, Switzerland, [7]Global Change Research Centre, ASCR, Brno, Czech Republic

Abstract We present a 1200 year drought reconstruction for the European Alpine region based on carbon isotope variations of tree rings from living larch trees and historic timber. The carbon isotope fractionation at the study site is sensitive to summer precipitation, temperature, and irradiance, resulting in a stable and high correlation with a drought index for interannual to decadal frequencies and possibly beyond ($r^2 = 0.58$ for 1901–2004, July/August). When combining this information with maximum latewood density-derived summer temperature, a strongly reduced occurrence of summer droughts during the warm A.D. 900–1200 period is evident, coinciding with the Medieval Climate Anomaly (MCA), with a shift to colder and drier conditions for the subsequent centuries. The warm-wet MCA contrasts strongly with the climate of the drought-prone warm phase of the recent decades, indicating different forcing mechanism for these two warm periods and pointing to beneficial conditions for agriculture and human well-being during the MCA in this region.

1. Introduction

Temperature reconstructions for medieval times are increasingly well constrained by many palaeorecords. The arguably Eurocentric observation of a "Medieval Warm Period" [*Hughes and Diaz*, 1994; *Lamb*, 1965] has been refined over the past decades into a global framework depicting spatially and temporally complex thermal and hydroclimatic variations [*Graham et al.*, 2011; *Mann et al.*, 2009]. Due to this heterogeneity, the term "Medieval Climate Anomaly" (MCA) is now preferred. This period from about A.D. 900 to 1350 is characterized, among others, by a prevalence of "La Niña-like" situations in the Pacific and positive modes of the North Atlantic Oscillation (NAO) [*Trouet et al.*, 2009]. However, our knowledge on precipitation and drought in general and particularly back to medieval times is still quite patchy and new records are urgently needed [*Seager et al.*, 2007]. The hydroclimate is well characterized in arid regions such as the western United States, showing extended droughts from A.D. 900 to 1250 [*Cook et al.*, 2004], as well as in southern Europe [*Esper et al.*, 2007]. Much less is known for moist temperate and northern regions, or partly conflicting data were reported, possibly due to the inherent high spatial variability of precipitation and different seasonal information retained in the different records. Evidence of wetter medieval times were reported for England based on historical documents [*Lamb*, 1965] and speleothem records [*Proctor et al.*, 2002], but other studies suggest a low occurrence of river floods in the Netherlands [*Tol and Langen*, 2000], strong drought in Finland [*Helama et al.*, 2009], or highly variable conditions in central Europe based on tree ring reconstructions [*Büntgen et al.*, 2011a, 2011b] and lake sediments [*Glur et al.*, 2013].

Recently, a drought reconstruction extending over 350 years was established for the Alps (Lötschental, Switzerland), a region where other proxy data for summer drought are scarce [*Kress et al.*, 2010]. This reconstruction was based on a high correlation of carbon isotope variations ($\delta^{13}C$) in the tree rings of larch (*Larix decidua*) from a high-altitude site with July-August drought, defined as the difference of precipitation and potential evapotranspiration ($P - PET$). Carbon isotope variations in plant matter and subsequently cellulose of trees are known to be influenced by dry conditions, as the diffusion of CO_2 through the stomatal pores determines (together with photosynthetic activity) the isotope discrimination [*Francey and Farquhar*, 1982].

In this study, we extend upon the previous reconstruction [*Kress et al*., 2010] with a focus on the MCA, by developing a continuous, well-replicated larch tree ring record of $\delta^{13}C$ back to A.D. 800.

2. Methods

Larch samples were collected in the Valais, southwestern Switzerland (46°26′N, 7°48′E). The recent period (1650–2004) is covered by living trees from the Lötschental (LOE-L), followed by two periods covered by historic material from buildings in the same region, LOE-H1 (1278–1700), and LOE-H2 (1180–1325), while the earliest period is covered by historic material from a building in Simplon Village (SIM-H; 800–1183), ~25 km from the other sites (all material from *Larix decidua*). For each period five dominant trees were chosen for isotope analysis (except for LOE-H2, where only four samples were available), a number generally considered to be satisfactory to provide a site-representative signal [*McCarroll and Loader*, 2004; *Treydte et al*., 2007]. To show consistency of the signals across the two regions (LOE versus SIM), additional samples were taken from living trees (i.e., "young" trees aged circa 150–250 years, five trees per site).

Tree ring width was measured and cross dated following standard procedures. The cores were split manually year-by-year using a scalpel. Each tree was analyzed separately in the calibration period (A.D. 1900–2004), while for the remaining period all cores were pooled prior to analysis for each annual ring, but retaining single-tree measurements every tenth year. The first 50 years of each core were not used [*McCarroll and Loader*, 2004]. Alpha cellulose was extracted from all samples [*Boettger et al*., 2007]. The carbon isotope ratio relative to the international standard Vienna Pee Dee belemnite ($\delta^{13}C$) was determined by mass spectrometry and corrected for the atmospheric decline in $\delta^{13}C$ due to fossil fuel burning since the beginning of the industrialization (by adding the difference between preindustrial and actual $\delta^{13}C$ for each year) [*Kress et al*., 2010].

The climate-isotope relationships were analyzed using the Swiss part of the HISTALP data set [*Auer et al*., 2007] in a detailed sensitivity study with the LOE-L material [*Kress et al*., 2009, 2010]. A drought index (DRI) was calculated as $DRI = P - PET$, where P is monthly precipitation and PET monthly potential evapotranspiration estimated according to *Thornthwaite* [1948]. Using linear regression, $\delta^{13}C$ values were calibrated to July-August DRI. To assess the predictive skill, a number of statistics were computed for independent calibration and verification periods [*Cook et al*., 1994; *Kress et al*., 2010]: (i) explained variance (R^2) of the regression models, (ii) the reduction of error (RE), (iii) coefficient of efficiency statistics (CE), where positive values indicate some degree of model skill, and (iv) the Durbin-Watson statistic (DW), where a value of 2 indicates no first-order autocorrelation in the residuals. In addition, EPS was calculated, indicating the Expressed Population Signal as a measure of the average correlation between the trees. Reconstruction errors were estimated by the root-mean-squared error (RMSE) of the prediction divided by the 51 year running RBAR of the carbon isotope series, which is defined as the average correlation between the trees in the respective 51 year window. The persistence in the isotope series was investigated by high- and low-pass filtering using cubic smoothing splines with a 50% frequency response cutoff at 10 and, alternatively, 20 years [*Cook and Peters*, 1981]. We determined the 100 most positive and negative isotope values of the entire period and compared them with the corresponding events in the maximum latewood density (MXD) series by *Büntgen et al*. [2006]. This MXD record consists of 180 larch samples, mainly collected in the Lötschental and Simplon region, and provides a strong summer temperature signal (June–September).

3. Results

Bootstrapped correlation coefficients between $\delta^{13}C$ and DRI for all months of the year and several seasonal windows for the period A.D. 1901–2004 (Figure 1) showed that highest correlations were obtained for the older trees (ages >350 years), typical of those incorporated into the final chronology. Young trees from the same site and trees from the Simplon region showed similar correlation strength and seasonal patterns. The highest values were obtained for July-August ($r = -0.76$), but significant values ($p < 0.001$) were also found for longer seasonal windows and even the annual average. Correlations with other climate variables such as temperature and radiation were also highly significant, albeit weaker [*Kress et al*., 2010]. Correlation coefficients for the relationship between raw, high- and low-passed $\delta^{13}C$, and DRI values over the twentieth century ranged from −0.75 to −0.82, indicating that (i) the signal is well balanced across different frequency domains and (ii) $\delta^{13}C$ can be used at least to reconstruct interannual up to multidecadal signals. Split period verification of the calibrated relationships for 1901–1952 and 1953–2004 indicated a reliable

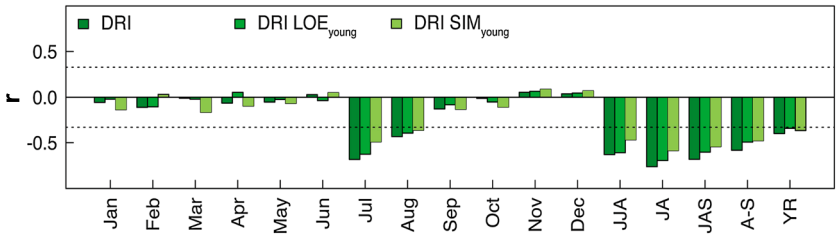

Figure 1. Bootstrapped climate correlation coefficients (*r*) for A.D. 1900–2004 for trees used in the chronology (DRI), young trees from the same site (DRI LOE_{young}), and young trees from the Simplon site (DRI SIM_{young}). Dotted lines represent confidence limits ($p < 0.001$).

model with high predictive skill ($r^2 = 0.62/0.54$, RE = 0.52/0.60, CE = 0.52/0.60, DW = 2.55/2.30). The reconstruction performance for the overall period 1900–2004 was similarly skillful ($r^2 = 0.58$, RSME = 0.64, DW = 2.49, $RBAR_{mean} = 0.76$, EPS = 0.94). *Kress et al.* [2010] used the same data to show that the reconstructed DRI is broadly consistent with instrumental data back to the seventeenth century.

The different cohorts of recent and historic material showed different absolute $\delta^{13}C$ levels of −23.54 ±0.27‰ for the recent part (LOE-L) and −22.65 ± 0.14‰ (LOE-H1), −21.59 ± 0.27‰ (LOE-H2), −22.94 ± 0.15‰ (SIM-H) for the historic material. These offsets render the linking of the cohorts challenging despite significant correlations in the overlapping periods [*Hangartner et al.*, 2012]. As matching the average $\delta^{13}C$ of the older cohort to the value of the newer one could produce artificial long-term trends [*Hangartner et al.*, 2012], or could only work if a very large number of trees was available for these periods [*Gagen et al.*, 2012], we linked the cohorts by standardizing each series to a mean of 0 and a standard deviation of 1 (but without any detrending involved). With this standardization, some loss of low-frequency information is undoubtedly involved, retaining variations up to the segment length of typically 350–400 years. However, we prefer this method to avoid unreliable long-term trends with the available tree replication, also considering that proxy reconstructions often overemphasize persistence compared to measured meteorological data [*Bunde et al.*, 2013; *Franke et al.*, 2013]. As a consequence, we focus our analysis and discussion mainly on the number of extremes, which should be less affected by the standardization.

The DRI reconstruction for A.D. 800–2004 shows pronounced alterations of drier and wetter periods (Figure 2). Remarkable features include the long absence of wet (summer) extremes from 1585 to 1706, reflecting a dry period, and a long period without dry (summer) events from 1107 to 1211, reflecting wet conditions. For the 1659–2000 period that we can compare with a previous monthly resolved multiproxy reconstruction [*Casty et al.*, 2005], we find that 79% of our predicted dry events were indeed relatively dry (i.e., below average of the DRI calculated from instrumental data), while 85% of the wet events were confirmed. The most extreme years predicted from our isotope data were not necessarily the most extreme based on the multiproxy reconstruction, but the top three driest summers (July/August) according to *Casty et al.* [2005] (1911, 1990, and 1991) were among the 17 driest in our reconstruction for the considered 341 year period (cf. Table S1 in the supporting information). This was not the case for the wettest summers, where we missed the "top three events" (1890, 1956, and 1960) according to *Casty et al.* [2005].

In Figures 3a–3c, we show the combined information obtained from the standardized carbon isotope series with the temperature-sensitive maximum latewood density (MXD) record from the Lötschental [*Büntgen*

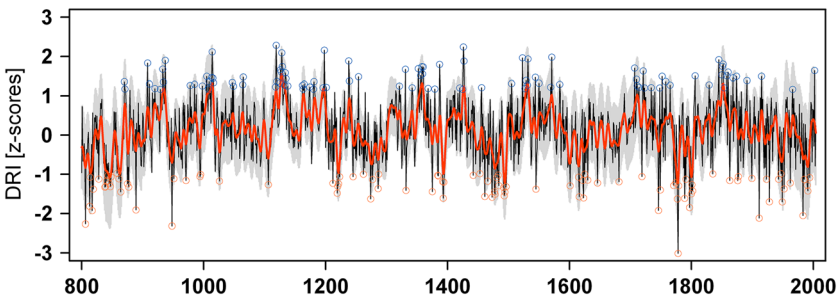

Figure 2. Drought reconstruction (DRI) based on $\delta^{13}C$ annually resolved and 10 year low pass filtered (red line) from the Lötschental, Swiss Alps. The gray shadow indicates the ± RMSE/RBAR error margin. The 100 driest (orange circles) and wettest (blue circles) years are highlighted.

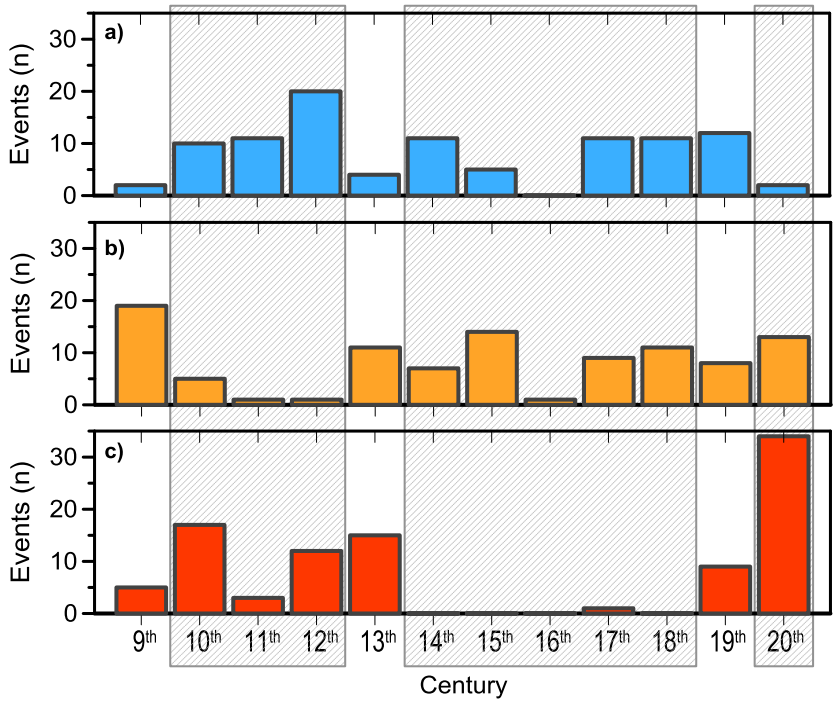

Figure 3. Number of extreme events per century for (a) $\delta^{13}C$ reflecting wet years, (b) dry years, and (c) maximum latewood density (MXD) representing warm years. For these data sets the 100 most positive values ($n = 100$) were chosen and added up for each century (21st century not shown in figure). Periods with differing climate patterns, roughly representing MCA (900–1200) and LIA (1300–1800), and the twentieth century, are marked with shaded areas.

et al., 2006]. Here the hundred most extreme warm, dry, and wet events over the entire record were identified and summed for each century. Noteworthy differences between the periods roughly representing MCA (900–1200) and Little Ice Age (LIA; 1300–1800) and the twentieth century are evident: The MCA is characterized by rather warm and wet conditions (unusually low occurrence of droughts), the LIA is characterized by an almost complete absence of warm events under relatively dry conditions, and the twentieth century features generally warm-dry conditions.

4. Discussion

We present a 1200 year summer drought reconstruction for the Alpine region, an area with limited hydroclimate information particularly prior to A.D. 1500 [*Casty et al*., 2005; *Seager et al*., 2007]. While tree growth at high-altitude sites such as in the Alps is generally not sensitive to precipitation [*Babst et al*., 2013], $\delta^{13}C$ in the cellulose of wood of larch trees is clearly sensitive to moisture deficit during the narrow July/August window (Figure 1). The carbon isotope ratio of organic matter depends on site conditions but typically contains a much stronger common signal both within a site and between proximal sites compared to ring width variation [*McCarroll and Loader*, 2004; *Saurer et al*., 2008]. The climate-driven common signal in cellulose $\delta^{13}C$ is principally well understood based on the fractionation during the diffusion of CO_2 into intercellular spaces, which is regulated by stomatal conductance [*Francey and Farquhar*, 1982]. However, it was surprising to find such a strong relationship to drought for a high-elevation site. This could be attributed to the combined influence of several interrelated climate variables during summer, all significantly related to $\delta^{13}C$, such that synoptic patterns simultaneously associated with high pressure, high sunshine, high temperature, low precipitation and low humidity promote relatively high $\delta^{13}C$, and vice versa for low-pressure systems [*Kress et al*., 2010].

We find, after an initial high occurrence of drought events in the ninth century, a pronounced period (A.D. 900–1200) with few dry extremes. This absence of droughts, in combination with a slightly enhanced number of wet extremes, suggests a relatively wet/warm period, roughly coinciding with the MCA. The MCA is confined to about A.D. 900–1350 [*Graham et al*., 2011] or, based on the retreats and advances of

glaciers in Europe, to A.D. 900–1300 [*Holzhauser et al*., 2005]. Some studies have suggested that a prevalence of a positive North Atlantic Oscillation (NAO), making Northern Europe wetter and the Mediterranean drier, may explain much of the medieval hydroclimate pattern in Europe [*Seager et al*., 2007; *Trouet et al*., 2009]. It is not straightforward to compare our drought reconstruction with these results, as first, the location in the Alps is intermediately relative to the dipole pattern of influence of the NAO, and second, the NAO is mainly a winter anomaly with relatively low impact on summer climate. Seasonal differences may also explain the differences from other reconstructions in Europe. Based on a large collection of historical oak samples from central Europe, mainly sensitive to spring conditions, *Büntgen et al*. [2011b] found—besides reduced climate variability around the MCA—relatively wet conditions in the tenth, thirteenth, and fourteenth centuries. This is somewhat similar to our results, although we find the wettest period from the tenth to the twelfth century. Furthermore, our reconstruction is broadly consistent with *Marcott et al*. [2013] who concluded that greater warmth was often associated with greater wetness during the Holocene in the extratropical Northern Hemisphere (>30°N).

The remarkable difference between MCA and LIA in our summer drought reconstruction is strikingly similar to published circulation anomalies. Our data suggest a wet/warm 900–1200 MCA period contrasting with the cool/dry centuries between 1300 and 1800, while the maximum of the LIA is confined to about 1500–1850. It has been suggested that "quasi-coordinated climate shifts" [*Graham et al*., 2011] were characteristic of many regions of the globe, caused by shifts in oceanic and atmospheric circulation patterns, thus resulting in the marked MCA-LIA differences, e.g., regarding the large-scale temperature development [*Frank et al*., 2010]. Global climate model simulations are able to portray similar patterns in both the spatial and temporal development of temperature [*Mann et al*., 2009]. Our data suggest that MCA-LIA variability also led to a dramatic change in moisture availability in the Alpine region.

Moreover, our data set points to a strong contrast between a warm/wet MCA and the warm/dry twentieth century. While the MCA has sometimes been used as an analog for a period of warmth comparable to the recent warming, it is quite clear that the mechanisms responsible for the MCA were very different from those that cause modern global warming [*Goosse et al*., 2012], including among others the strong CO_2 increase. This is confirmed by our results of clearly differing climate regimes between the MCA and the recent period. Droughts can have a tremendous impact on ecosystems [*Allen et al*., 2010], with increased evidence that major cultural changes are often related to climate changes [*Büntgen et al*., 2011b; *Hsiang et al*., 2013]. Our $\delta^{13}C$-based reconstruction fills a data gap for the hydroclimatic changes prior to A.D. 1500 and adds new details to the picture of spatiotemporal climate patterns in the past. The causes of climate change in the preinstrumental period can be understood better only when precipitation or drought information is included in models so as to go beyond the more widely available temperature-only reconstructions.

Acknowledgments

This study was supported by the EC project MILLENNIUM (FP6-2004-GLOBAL-017008-2) and the Swiss National Science Foundation projects iTREE and 200020_134864. U.B. was additionally supported by the Operational Programme of Education for Competitiveness of Ministry of Education, Youth and Sports of the Czech Republic (project CZ.1.07/2.3.00/20.0248). The authors thank two anonymous reviewers for their constructive comments.

The Editor thanks two anonymous reviewers for their assistance in evaluating this paper.

References

Allen, C. D., et al. (2010), A global overview of drought and heat-induced tree mortality reveals emerging climate change risks for forests, *For. Ecol. Manage.*, *259*(4), 660–684.

Auer, I., et al. (2007), HISTALP—Historical instrumental climatological surface time series of the Greater Alpine Region, *Int. J. Climatol.*, *27*(1), 17–46.

Babst, F., et al. (2013), Site- and species-specific responses of forest growth to climate across the European continent, *Global Ecol. Biogeogr.*, *22*, 706–717.

Boettger, T., et al. (2007), Wood cellulose preparation methods and mass spectrometric analyses of $\delta^{13}C$, $\delta^{18}O$, and nonexchangeable $\delta^{2}H$ values in cellulose, sugar, and starch: An interlaboratory comparison, *Anal. Chem.*, *79*(12), 4603–4612.

Bunde, A., U. Büntgen, J. Ludescher, J. Luterbacher, and H. von Storch (2013), Is there memory in precipitation?, *Nat. Clim. Change*, *3*(3), 174–175.

Büntgen, U., D. C. Frank, D. Nievergelt, and J. Esper (2006), Summer temperature variations in the European Alps, AD 755–2004, *J. Clim.*, *19*(21), 5606–5623.

Büntgen, U., R. Brazdil, K.-U. Heussner, J. Hofmann, R. Kontic, T. Kyncl, C. Pfister, K. Chroma, and W. Tegel (2011a), Combined dendro-documentary evidence of Central European hydroclimatic springtime extremes over the last millennium, *Quat. Sci. Rev.*, *30*(27–28), 3947–3959.

Büntgen, U., et al. (2011b), 2500 years of European climate variability and human susceptibility, *Science*, *331*(6017), 578–582.

Casty, C., H. Wanner, J. Luterbacher, J. Esper, and R. Böhm (2005), Temperature and precipitation variability in the European Alps since 1500, *Int. J. Climatol.*, *25*(14), 1855–1880.

Cook, E. R., and K. Peters (1981), The smoothing spline: A new approach to standardizing forest interior tree-ring width series for dendroclimatic studies, *Tree Ring Bull.*, *41*, 45–53.

Cook, E. R., K. R. Briffa, and P. D. Jones (1994), Spatial regression methods in dendroclimatology: A review and comparison of 2 techniques, *Int. J. Climatol.*, *14*, 379–402.

Cook, E. R., C. A. Woodhouse, C. M. Eakin, D. M. Meko, and D. W. Stahle (2004), Long-term aridity changes in the western United States, *Science*, *306*(5698), 1015–1018.

Esper, J., D. Frank, U. Büntgen, A. Verstege, and J. Luterbacher (2007), Long-term drought severity variations in Morocco, *Geophys. Res. Lett.*, *34*, L17702, doi:10.1029/2007GL030844.
Francey, R. J., and G. D. Farquhar (1982), An explanation of $^{13}C/^{12}C$ variations in tree rings, *Nature*, *297*(5861), 28–31.
Frank, D. C., J. Esper, C. C. Raible, U. Büntgen, V. Trouet, B. Stocker, and F. Joos (2010), Ensemble reconstruction constraints on the global carbon cycle sensitivity to climate, *Nature*, *463*(7280), 527–U143.
Franke, J., D. Frank, C. C. Raible, J. Esper, and S. Broennimann (2013), Spectral biases in tree-ring climate proxies, *Nat. Clim. Change*, *3*(4), 360–364.
Gagen, M., D. McCarroll, R. Jalkanen, N. J. Loader, I. Robertson, and G. H. F. Young (2012), A rapid method for the production of robust millennial length stable isotope tree ring series for climate reconstruction, *Glob. Planet. Change*, *82–83*, 96–103.
Glur, L., S. B. Wirth, U. Büntgen, A. Gilli, G. H. Haug, C. Schär, J. Beer, and F. S. Anselmetti (2013), Frequent floods in the European Alps coincide with cooler periods of the past 2500 years, *Sci. Rep.*, *3*, 2770, doi:10.1038/srep02770.
Goosse, H., E. Crespin, S. Dubinkina, M.-F. Loutre, M. E. Mann, H. Renssen, Y. Sallaz-Damaz, and D. Shindell (2012), The role of forcing and internal dynamics in explaining the "Medieval Climate Anomaly", *Clim. Dyn.*, *39*(12), 2847–2866.
Graham, N. E., C. M. Ammann, D. Fleitmann, K. M. Cobb, and J. Luterbacher (2011), Support for global climate reorganization during the "Medieval Climate Anomaly", *Clim. Dyn.*, *37*(5–6), 1217–1245.
Hangartner, S., A. Kress, M. Saurer, D. C. Frank, and M. Leuenberger (2012), Methods to merge overlapping tree-ring isotope series to generate multi-centennial chronologies, *Chem. Geol.*, *294*(295), 127–134.
Helama, S., J. Merilainen, and H. Tuomenvirta (2009), Multicentennial megadrought in northern Europe coincided with a global El Niño-Southern Oscillation drought pattern during the Medieval Climate Anomaly, *Geology*, *37*(2), 175–178.
Holzhauser, H., M. Magny, and H. J. Zumbuhl (2005), Glacier and lake-level variations in west-central Europe over the last 3500 years, *Holocene*, *15*(6), 789–801.
Hsiang, S. M., M. Burke, and E. Miguel (2013), Quantifying the influence of climate on human conflict, *Science*, *341*(6151), 1235367, doi:10.1126/science.1235367.
Hughes, M. K., and H. F. Diaz (1994), Was there a "Medieval Warm Period", and if so, where and when?, *Clim. Change*, *26*(2–3), 109–142.
Kress, A., M. Saurer, U. Büntgen, K. S. Treydte, H. Bugmann, and R. T. W. Siegwolf (2009), Summer temperature dependency of larch budmoth outbreaks revealed by Alpine tree-ring isotope chronologies, *Oecologia*, *160*(2), 353–365.
Kress, A., M. Saurer, R. T. W. Siegwolf, D. C. Frank, J. Esper, and H. Bugmann (2010), A 350 year drought reconstruction from Alpine tree ring stable isotopes, *Global Biogeochem. Cycles*, *24*, GB2011, doi:10.1029/2009GB003613.
Lamb, H. H. (1965), The early medieval warm epoch and its sequel, *Palaeogeogr. Palaeoclimatol. Palaeoecol.*, *1*, 13–37.
Mann, M. E., Z. Zhang, S. Rutherford, R. S. Bradley, M. K. Hughes, D. Shindell, C. Ammann, G. Faluvegi, and F. Ni (2009), Global signatures and dynamical origins of the Little Ice Age and Medieval Climate Anomaly, *Science*, *326*(5957), 1256–1260.
Marcott, S. A., J. D. Shakun, P. U. Clark, and A. C. Mix (2013), A reconstruction of regional and global temperature for the past 11,300 years, *Science*, *339*(6124), 1198–1201.
McCarroll, D., and N. J. Loader (2004), Stable isotopes in tree rings, *Quat. Sci. Rev.*, *23*(7–8), 771–801.
Proctor, C. J., A. Baker, and W. L. Barnes (2002), A three thousand year record of North Atlantic climate, *Clim. Dyn.*, *19*(5–6), 449–454.
Saurer, M., P. Cherubini, C. E. Reynolds-Henne, K. S. Treydte, W. T. Anderson, and R. T. W. Siegwolf (2008), An investigation of the common signal in tree ring stable isotope chronologies at temperate sites, *J. Geophys. Res.*, *113*, G04035, doi:10.1029/2008JG000689.
Seager, R., N. Graham, C. Herweijer, A. L. Gordon, Y. Kushnir, and E. Cook (2007), Blueprints for Medieval hydroclimate, *Quat. Sci. Rev.*, *26*(19–21), 2322–2336.
Thornthwaite, C. W. (1948), An approach toward a rational classification of climate, *Geogr. Rev.*, *38*, 55–94.
Tol, R. S. J., and A. Langen (2000), A concise history of Dutch river floods, *Clim. Change*, *46*(3), 357–369.
Treydte, K., et al. (2007), Signal strength and climate calibration of a European tree-ring isotope network, *Geophys. Res. Lett.*, *34*, L24302, doi:10.1029/2007GL031106.
Trouet, V., J. Esper, N. E. Graham, A. Baker, J. D. Scourse, and D. C. Frank (2009), Persistent positive North Atlantic Oscillation mode dominated the Medieval Climate Anomaly, *Science*, *324*(5923), 78–80.